Effect of Molecular Weight on the Rheological Behavior of Thermotropic Liquid-Crystalline Polymer

Seung Su Kim and Chang Dae Han*

Department of Chemical Engineering, Polytechnic University, Brooklyn, New York 11201

Received May 13, 1993; Revised Manuscript Received August 23, 1993•

ABSTRACT: The effect of molecular weight on the rheological behavior of a thermotropic liquid-crystalline polymer was investigated. For the study, an aromatic polyester, poly[(phenylsulfonyl)-*p*-phenylene 1,10-decamethylenebis(4-oxybenzoate)] (PSHQ10) having different molecular weights was synthesized. The PSHQ10s synthesized were found to have (a) a weight-average molecular weight (M_w), as determined by gel permeation chromatography, ranging from 33 000 to 45 000 relative to polystyrene standards, and a polydispersity index of about 2, and (b) a melting point ranging from 100 to 115 °C and a nematic-to-isotropic transition temperature ranging from 161 yo 176 °C, depending upon the molecular weight. Using a cone-and-plate rheometer, the steady and oscillatory shear flow properties of the PSHQ10s were measured in both the *isotropic* and *nematic* regions. We found that (a) $\eta_0 \propto M^{6.5}$ and negligible N_1 in the *isotropic* region, and (b) $\eta_0 \propto M^6$ and $N_1 \propto M^{6.7}$ in the *nematic* region, where M is the molecular weight, η_0 is the zero-shear viscosity, and N_1 is the first normal stress difference. We found further that *preshearing* has a profound influence on both the steady and oscillatory shear properties of PSHQ10. Also investigated were the transient start-up shear flow, stress relaxation, and structural recovery after cessation of steady shear flow. Structural recovery was determined by monitoring the variations of dynamic storage and loss moduli, during application of small-amplitude oscillatory deformations to the specimens. The following observations were made: (1) the maximum overshoot in both shear stress and the first normal stress difference increased with increasing molecular weight; (2) the rate of stress relaxation after cessation of shear flow was slower with increasing molecular weight; and (3) the extent of structural recovery after cessation of shear flow was greater for increasing molecular weight.

Introduction

In recent years, the rheological behavior of thermotropic liquid-crystalline polymers (TLCPs) has attracted much attention from rheologists.[1–16] However, very *little* experimental study has been reported on the effect of molecular weight on the rheological behavior of TLCPs, while the dependence of shear viscosity on molecular weight for some lyotropic liquid-crystalline polymers (LLCPs) has been reported.[17] Over a decade ago, Doi[18] developed a molecular theory which predicts that the molecular weight has a much greater influence on the rheological properties of rigid-rod-like macromolecules than on the rheological properties of flexible homopolymers. Note that for entangled flexible homopolymers the zero-shear viscosity (η_0) varies with the 3.4th power of molecular weight, and the first normal stress difference (N_1) varies with the 6–7th power of molecular weight.[19,20]

In our previous studies,[21–24] using an aromatic polyester, poly[(phenylsulfonyl)-*p*-phenylene 1,10-decamethylenebis(4-oxybenzoate)] (PSHQ10)

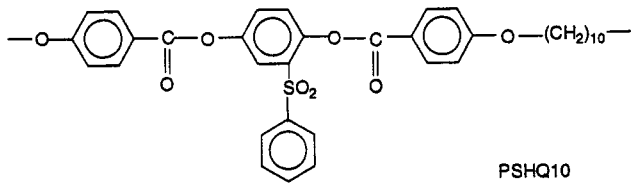

PSHQ10

with the repeat unit structure which had a weight-average molecular weight of about 45 000 relative to polystyrene standards, we investigated (a) the effect of thermal history on its rheological behavior, (b) transient start-up shear flow, (c) steady shear flow behavior, and (d) oscillatory shear flow behavior. This polymer, having a melting point of 115 °C and a nematic-to-isotropic transition temperature (T_{NI}) of 175 °C, enabled us to investigate its rheological behavior in both the isotropic and nematic states, without being concerned about the possibility of having thermal degradation at about 350 °C.

As part of our ongoing research effort on enhancing our understanding of the rheology of TLCPs, very recently we synthesized PSHQ10 having several different molecular weights and then investigated the effect of molecular weight on its rheological behavior. In the present paper, we shall report the highlights of our findings, namely, the effect of the molecular weight of PSHQ10 on (1) transient start-up shear flow behavior in the *nematic* region, (2) steady and oscillatory shear flow behavior in both the *isotropic* and *nematic* regions, (3) stress relaxation upon cessation of steady shear flow, and (4) structural recovery after cessation of steady shear flow.

Table I. Summary of the Molecular Weight and Intrinsic Viscosity of the PSHQ10s Synthesized in This Study

sample code	$M_w \times 10^{-3}$	M_w/M_n	$[\eta]$ (dL/g)
A	53.4	1.89	0.616
B	49.5	2.03	0.560
C	45.2	2.11	0.500
D	38.9	2.48	0.432
E	37.6	2.43	0.409
F	35.0	2.09	0.387

Experimental Section

Materials and Molecular Characteristics. Six PSHQ10s having different molecular weights were synthesized using the procedures described in previous papers.[24,25] The readers are referred to the original papers for the details of the method of synthesis. The weight-average molecular weight (M_w) of the PSHQ10s synthesized was determined via gel permeation chromatography using polystyrene standards, and Table I gives sample codes and a summary of M_w for the six PSHQ10s synthesized in this study.

* To whom correspondence should be addressed at the Department of Polymer Engineering and Institute of Polymer Engineering, The University of Akron, Akron, OH 44325.

• Abstract published in *Advance ACS Abstracts*, October 15, 1993.

0024-9297/93/2226-6633$04.00/0

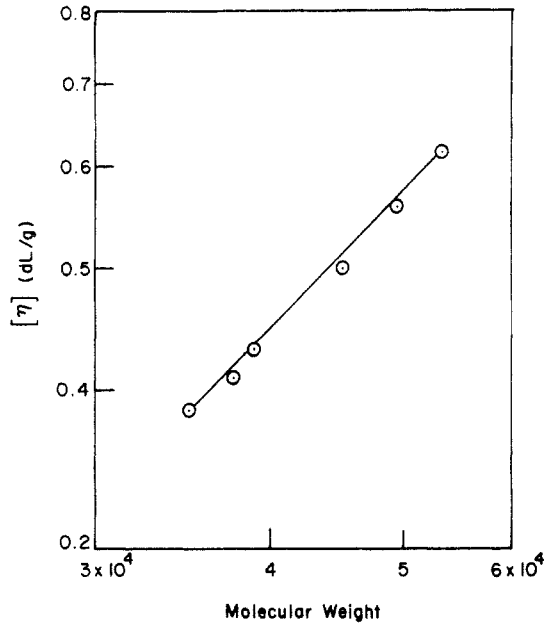

Figure 1. Plots of $[\eta]$ versus M_w for PSHQ10, where THF was used as solvent in the measurements of molecular weight via GPC at 25 °C.

We also measured the intrinsic viscosity $[\eta]$ of each polymer sample dissolved in trichlorobenzene at 70 °C. Plots of log $[\eta]$ versus log M_w for the six PSHQ10s synthesized are given in Figure 1. Using the data given in Figure 1 we obtain the Mark–Houwink relationship, $[\eta] = KM^a$, where $K = 3.7 \times 10^{-6}$ and $a = 1.1$ for a pair of PSHQ10 and trichlorobenzene at 70 °C. Owing to the polydisperse nature of the PSHQ10 samples, in the Mark–Houwink equation we employed the weight-average molecular weight (M_w), which is much closer to the viscosity-average molecular weight (M_v), than the number-average molecular weight (M_n). In view of the fact that the value of the exponent a in the Mark–Houwink equation is known to lie between 0.5 and 0.8, depending on the solvating power of the medium, for flexible polymer chains, the value of $a = 1.1$ for PSHQ10, which is a semiflexible polymer, seems to be reasonable. We hasten to point out, however, that we are well aware of the fact that the hydrodynamic volume of PSHQ10 is not the same as flexible homopolymers.

Sample Preparation. Specimens for rheological and DSC measurements were prepared by first dissolving PSHQ10 in dichloromethane in the presence of an antioxidant (Irganox 1010; Ciba-Geigy Group) and then slowly evaporating the solvent at room temperature for a week. The cast films with a thickness of 1 mm were further dried in a vacuum oven at room temperature for at least 3 weeks and at 90 °C for 48 h. Right before the rheological measurements, the specimen was further dried at 120 °C for 2 h to remove any residual solvent and moisture.

Differential Scanning Calorimetry. The thermal transition of PSHQ10 was determined using differential scanning calorimetry (DSC) with a heating rate of 20 °C/min. Figure 2 gives DSC traces for six PSHQ10 samples having different molecular weights during the first heating cycle after the polymers were annealed at 190 °C for 5 min. It can be seen in Figure 2 that both the melting point and nematic-to-isotropic transition temperature (T_{NI}) increase with increasing molecular weight. Earlier, a similar observation was reported for other types of TLCPs.[26-30]

Rheological Measurement. A Model R16 Weissenberg rheogoniometer (Sangamo Control, Inc.) in the cone-and-plate (25-nm-diameter plate and 4° cone angle) configuration was used to measure in the steady shear mode the shear viscosity (η) and first normal stress difference (N_1) as functions of shear rate ($\dot{\gamma}$) and in the oscillatory mode the dynamic storage modulus (G') and dynamic loss modulus (G'') as functions of angular frequency (ω) in both the *isotropic* and *nematic regions*. The absolute values of complex viscosity were calculated using $|\eta^*| = [(G'(\omega)/\omega)^2 + (G''(\omega)/\omega)^2]^{1/2}$. Data acquisition was accomplished with the aid of a microcomputer interfaced with the rheometer. All experiments were conducted in the presence of nitrogen in order to preclude oxidative degradation of the specimen. Temperature control was satisfactory to within ±1 °C.

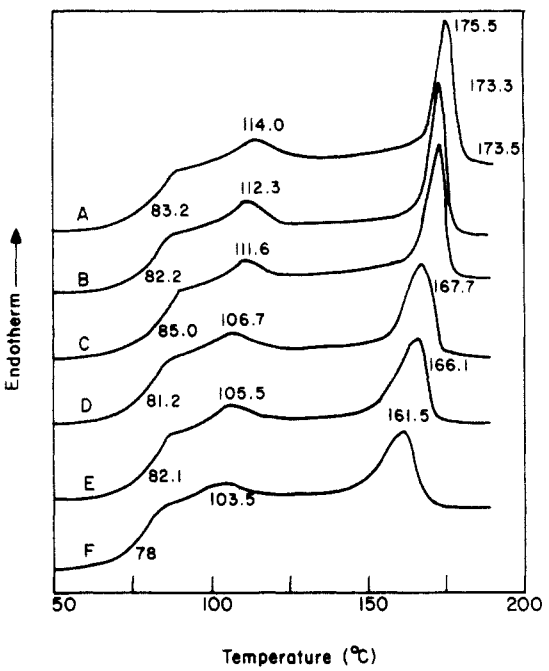

Figure 2. DSC traces for as-cast PSHQ10 samples (see Table I for sample code), which were annealed for 5 min at 190 °C, showing the glass transition temperature, melting point, and nematic-to-isotropic transition temperature.

In order to be able to obtain reproducible initial conditions in the nematic region, we employed the following temperature protocols. First, an as-cast PSHQ10 specimen was placed between the cone and plate after the fixture was heated to 190 °C, which is at least 15 °C above the T_{NI} of PSHQ10. After the temperature was equilibrated at 190 °C which took about 5 min upon placement of a specimen, steady shear flow at rates ranging from 0.0085 to 1.07 s^{-1} was applied to the specimen for 5 min at each shear rate by which time the shear stress had attained a constant value. We then cooled the specimen very slowly to a predetermined temperature in the nematic state (i.e., 130, 140, 150, or 160 °C). After temperature equilibration at the desired level in the nematic state, we applied a sudden shear flow to the specimen and then the growths of shear stress $\sigma^+(t,\dot{\gamma})$ and first normal stress difference $N_1^+(t,\dot{\gamma})$ were recorded on a chart recorder until both leveled off. After a steady state was attained, the flow was stopped and then "structural recovery" was monitored from measurements of the dynamic moduli (G' and G'') by applying small-amplitude oscillatory deformations to the specimen.

Results and Discussion

Molecular Weight Dependence of Steady Shear Viscosity of PSHQ10 in the Isotropic Region. In the present study both the steady and oscillatory shear flow properties of PSHQ10 in the *isotropic* state (at 190 °C) were measured. Figure 3 gives plots of log η versus log $\dot{\gamma}$, and plots of log $|\eta^*|$ versus low ω, for five PSHQ10 samples, A–E. We observe in Figure 3 that the Cox–Merz rule[31] holds for the PSHQ10 samples, which is a manifestation that these samples are indeed in the *isotropic* state. It should be mentioned that negligible values for N_1 were detected for these samples.

Figure 4 gives logarithmic plots of zero-shear viscosity (η_0) versus M_w for the five PSHQ10 samples, from which we obtain via regression analysis the following relationship:[32]

$$\eta_0 \propto M^{6.5} \quad (1)$$

We hasten to add that, in view of the fact that in this study variations of molecular weight were rather small

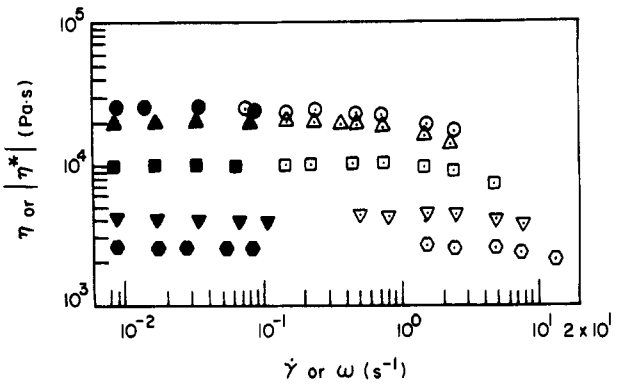

Figure 3. Plots of log η versus log $\dot{\gamma}$ (open dotted symbols), and log $|\eta^*|$ versus log ω (filled symbols), for PSHQ10 samples in the isotropic region at 190 °C: (⊙,●) sample A; (▲,▲) sample B; (⊡,■) sample C; (▼,▼) sample D; (⊙,●) sample E.

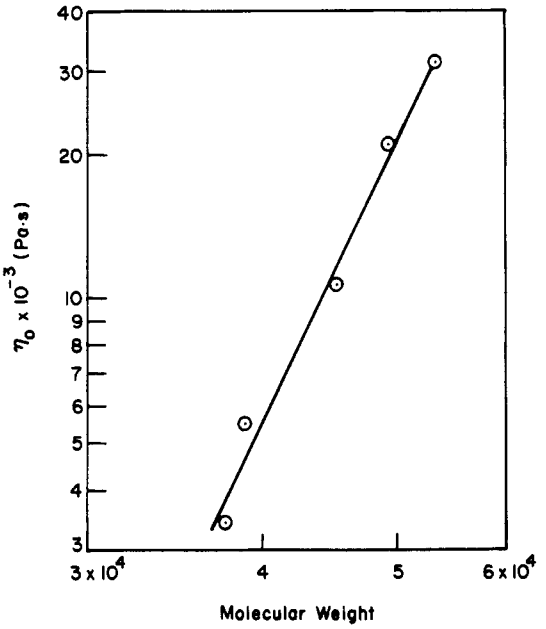

Figure 4. Plots of log η_0 in the isotropic region at 190 °C versus M_w for PSHQ10 samples.

(35 000–53 000), the 6.5th power of molecular weight given in eq 1 must be regarded as an approximation. Notice in Figure 3 that the η_0 increased by an order of magnitude as the molecular weight increased only by 45%. According to eq 1, the η_0 would be increased by 90 times if the molecular weight is doubled and by 1260 times if the molecular weight is tripled. For such viscous liquids, it would be very difficult to measure their viscosities, and thus there is a practical limitation to the extent of variation of molecular weight that one can make from the point of rheological measurement.

It should be mentioned that earlier Doi[18,33,34] predicted the relationship $\eta_0 \propto M^6$ for the *isotropic* phase of rigid-rod-like macromolecules. In view of the fact that PSHQ10 is a semiflexible macromolecule having decamethylene units as a flexible spacer in the main chain, we can conclude that, within experimental uncertainties, the experimental results for the dependence of η_0 on M presented above are in reasonable agreement with the Doi theory.

Figure 5 gives plots of log G' versus log ω, and plots of log G'' versus log ω, for five PSHQ10 samples at 190 °C. It can be seen in Figure 5 that the frequency dependencies of G' and G'' are very similar to those usually observed for flexible homopolymers in the molten state; namely, in the terminal region, $G' \propto \omega^2$ and $G'' \propto \omega$. Notice in Figure 5 that the values of G' and G'' increase with increasing

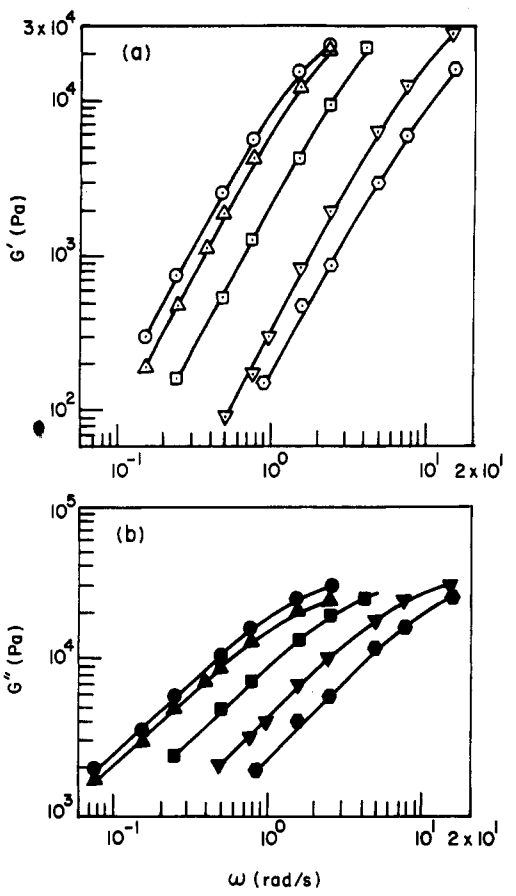

Figure 5. (a) Plots of log G' versus log ω (open dotted symbols) and (b) plots of log G'' versus log ω (filled symbols) in the isotropic region at 190 °C for PSHQ10 samples: (⊙,●) sample A; (▲,▲) sample B; (⊡,■) sample C; (▼,▼) sample D; (⊙,●) sample E.

molecular weight of PSHQ10, consistent with the observations made for flexible homopolymers.[19]

Figure 6 gives plots of log G' versus log G'' for five PSHQ10 samples, which were prepared with the data given in Figure 5. It is of interest to observe in Figure 6 that the dependence of molecular weight is not discernible in such plots, having a slope of 2 in the terminal region. Using a molecular viscoelasticity theory for *entangled* flexible homopolymers, Han and Jhon[35] have shown that plots of log G' versus log G'' in the *terminal* region are independent of molecular weight, and indeed such a prediction was proven to be valid by experimental results. Therefore, we can conclude from Figure 6 that the five PSHQ10 samples investigated here have molecular weights greater than the *entanglement* molecular weight, although we recognize the fact that in the strict sense the Han–Jhon theory is valid only for flexible macromolecules. It can be easily shown that, using the Rouse model, log G' versus log G'' plots for *unentangled* flexible homopolymers would show molecular weight dependency.[36]

Control of Initial Conditions for PSHQ10 in the Nematic Region. In the measurement of the rheological properties of a TLCP in the *nematic* region, it is of utmost importance for one to be able to control *initial conditions*, so that measurements can be reproducible. It was shown earlier that, unless extraordinary precautions are taken, the rheological properties of a TLCP may change during the measurements.[21,37] In our previous paper[21] we showed that the rheological behavior of PSHQ10 in the *nematic* region was very sensitive to thermal history and that thermal treatment in the isotropic state under steady shear flow was a very effective way to control initial conditions (thus we were able to obtain reproducible data) for

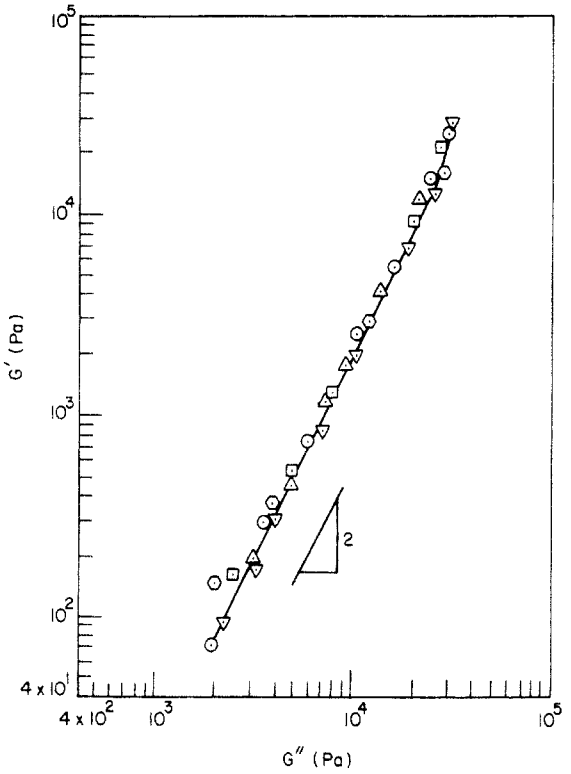

Figure 6. Plots of log G' versus log G'' in the isotropic region at 190 °C for PSHQ10 samples: (⊙) sample A; (▲) sample B; (⊡) sample C; (▽) sample D; (⊙) sample E.

PSHQ10 in the *nematic* region. In the present study we employed a specific temperature protocol, as described in the Experimental Section, to control initial conditions for the five PSHQ10 samples in the *nematic* region. That is, before proceeding to the application of a sudden shear flow to the specimen in the *nematic* region, we confirmed that values of $|\eta^*|$, which were obtained by applying small-amplitude oscillatory deformations at ω = 0.15 rad/s, remained more or less constant for about 50 h, indicating that the initial morphology established would vary little during subsequent shear flow experiments.

Figure 7 gives plots of log G' versus log ω, and plots of log G'' versus log ω, for five PSHQ10 samples at 140 °C. Of particular note is the dependence of G' on ω in the *nematic* region, which is much weaker than that in the *isotropic* region, while the dependence of G'' on ω appears to be about the same in both the *nematic* and *isotropic* regions (compare Figure 7 with Figure 5). This points out the fact that the elastic property of PSHQ10 is much more sensitive to the applied angular frequency than is the viscous property.

Using the data displayed in Figure 7, we prepared plots of log G' versus log G'' for the PSHQ10s in the *nematic* state at 140 °C (open symbols), and they are given in Figure 8. Also given in Figure 8 are, for comparison, plots of log G' versus log G'' for the five PSHQ10 samples in the *isotropic* state at 190 °C (filled symbols). The following observations are worth noting in Figure 8. (1) Plots of log G' veruss log G'' in the *nematic* region (open symbols) are seen to lie on a single correlation, independent of molecular weight. Recall that for *entangled* polymers log G' versus log G'' plots are expected to be independent of molecular weight. This certainly suggests that the morphological states of the five samples are *virtually* identical at the measurement temperature (140 °C), in spite of the fact that each sample was first thermally treated separately in the isotropic region at 190 °C and then cooled slowly down to the nematic region at 140 °C. This attests to the fact

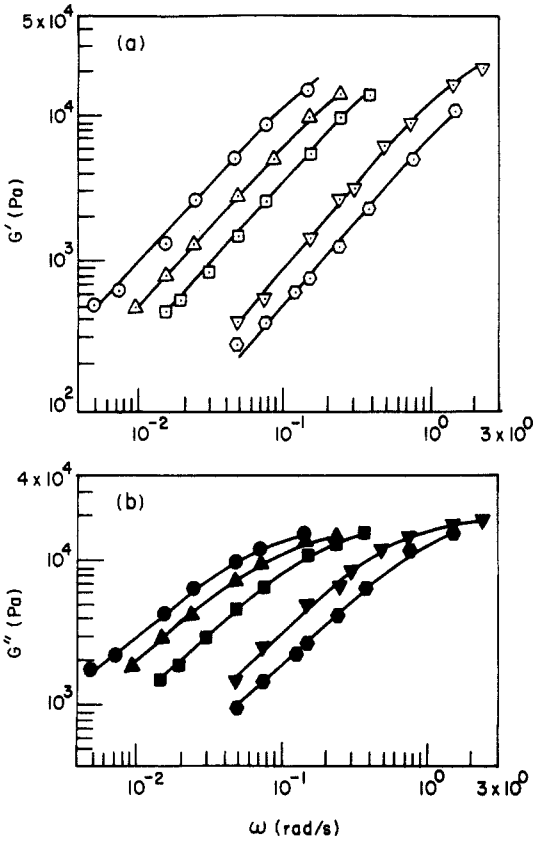

Figure 7. (a) Plots of log G' versus log ω (open dotted symbols) and (b) plots of log G'' versus log ω (filled symbols) in the nematic region at 140 °C for PSHQ10 samples before being subjected to steady shear flow: (⊙,●) sample A; (▲,▲) sample B; (⊡,■) sample C; (▽,▼) sample D.; (⊙,●) sample E.

that the initial conditions for the samples were well controlled by the temperature protocols employed in this study. (2) In the terminal region, the slope of log G' versus log G'' plots is much *less* than 2 in the *nematic* region (open symbols), while it is very close to 2 in the *isotropic* region (filled symbols). Similar observations were made earlier by Han and co-workers,[38-40] who investigated the dynamic viscoelastic properties of block copolymers in the ordered and disordered states. Thus, the results in Figure 8 lead us to conclude that log G' versus log G'' plots are very sensitive to the morphological state of PSHQ10 (also other TLCPs as well). It should be mentioned that in a previous paper[22] we showed that log G' versus log G'' plots for PSHQ10 in the *nematic* state vary with temperature, while such plots are independent of temperature for PSHQ10 in the *isotropic* region.

Effect of Molecular Weight on the Start-Up Shear Flow of PSHQ10 in the Nematic Region. Having shown how we controlled initial conditions, let us now examine how the molecular weight affected the transient start-up shear flow of PSHQ10. Figure 9 gives plots of shear stress growth $\sigma^+(t,\dot{\gamma})$ versus $\dot{\gamma}t$, and Figure 10 gives plots of the first normal stress difference growth $N_1^+(t,\dot{\gamma})$ versus $\dot{\gamma}t$, for five PSHQ10 samples at 140 °C for a shear rate of 0.536 s^{-1}, where $\dot{\gamma}$ is shear rate and t is time. The following observations are worth noting in Figures 9 and 10. (1) The maximum overshoot in $\sigma^+(t,\dot{\gamma})$ increases with increasing molecular weight of PSHQ10, and that multiple overshoots of $\sigma^+(t,\dot{\gamma})$ appear as the molecular weight of PSHQ10 becomes greater than a certain critical value. (2) The appearance of multiple overshoots in $N_1^+(t,\dot{\gamma})$ is very pronounced with increasing molecular weight of PSHQ10, and that the value of $\dot{\gamma}$ at which the first overshoot of $N_1^+(t,\dot{\gamma})$ occurs increases with increasing molecular weight

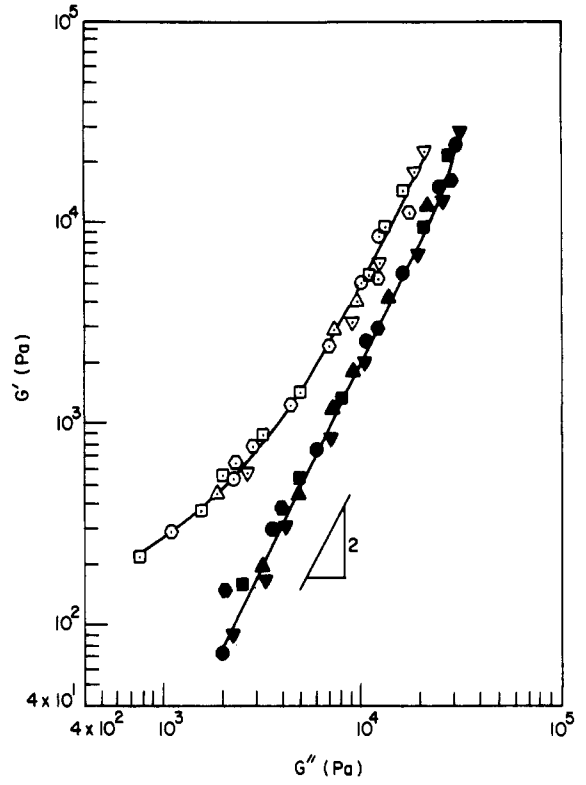

Figure 8. Plots of log G' versus log G'' for PSHQ10 samples. (a) At 140 °C: (⊙) sample A; (▲) sample B; (⊡) sample C; (▼) sample D; (⊙) sample E. (b) At 190 °C (●) sample A; (▲) sample B; (■) sample C; (▼) D; (●) sample E.

(i.e., the higher the molecular weight of PSHQ10, the longer it takes for the maximum of the first overshoot of $N_1^+(t,\dot{\gamma})$ to appear). Notice further in Figure 10 that there is only a single overshoot of $N_1^+(t,\dot{\gamma})$ occurring for molecular weights below a certain critical value. (3) The time required for $N_1^+(t,\dot{\gamma})$ to reach steady state is much longer than that for $\sigma^+(t,\dot{\gamma})$. We hasten to point out, however, that according to the results of our previous study,[22] the number of overshoots appearing in $N_1^+(t,\dot{\gamma})$ does not only depend on applied shear rate.

Figure 11 describes the effect of temperature on $\sigma^+(t,\dot{\gamma})$, and Figure 12 describes the effect of temperature on $N_1^+(t,\dot{\gamma})$, for sample C at $\dot{\gamma} = 0.536\ s^{-1}$ for 130, 140, and 150 °C. It can be seen in Figures 11 and 12 that while the value of $\dot{\gamma}t$ at which a maximum in $\sigma^+(t,\dot{\gamma})$ appears is relatively insensitive to temperature, the value of the maximum $\sigma^+(t,\dot{\gamma})$ becomes greater as the temperature decreases. These observations seem to suggest to us that, as the temperature of PSHQ10 moves farther away from the T_{NI}, greater shear stresses are required to break up polydomains, which existed in the specimen before being subjected to a start-up shear flow. It is of interest to observe in Figure 12 that the magnitude of the first overshoot of $N_1^+)t,\dot{\gamma})$ increases with decreasing temperature and that a much longer time is required for $N_1^+(t,\dot{\gamma})$ to reach steady state as the temperature decreases (i.e., as the temperature of PSHQ10 moves farther away from the T_{NI}). From Figures 11 and 12 we can conclude that both shear rate and temperature have profound influences on the transient shear flow behavior of PSHQ10.

We observe from Figures 9–12 that the ratio of the maximum peak to the equilibrium value of shear stress, $\sigma_{max}/\sigma_\infty$, lies between 8 and 12, and the ratio of the maximum peak to the equilibrium value of the first normal stress difference, $N_{1,max}/N_{1,\infty}$, lies between 2.5 and 3.5, depending upon the applied shear rate and measurement temperature. Such unusually large values of overshoot in

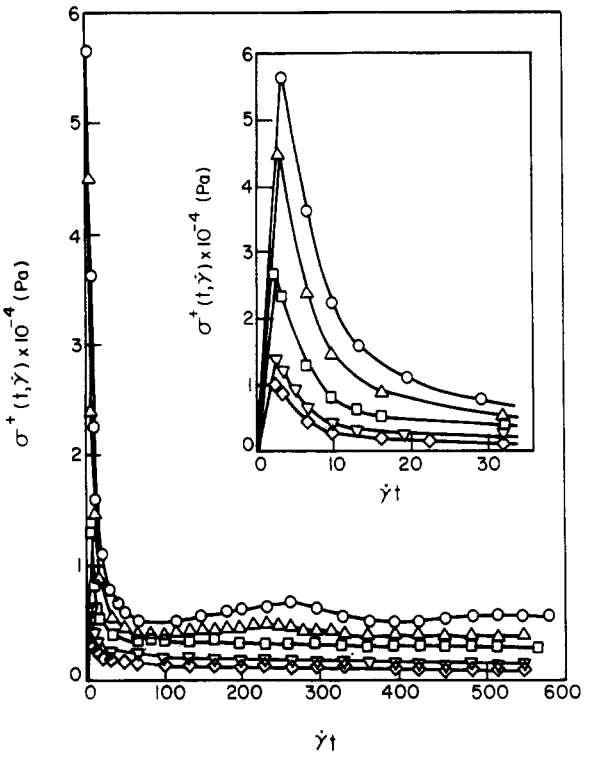

Figure 9. Plots of $\sigma^+(t,\dot{\gamma})$ versus $\dot{\gamma}t$ for PSHQ10 samples at 140 °C for $\dot{\gamma} = 0.536\ s^{-1}$: (○) sample A; (△) sample B; (□) sample C; (▽) sample D; (◇) sample E.

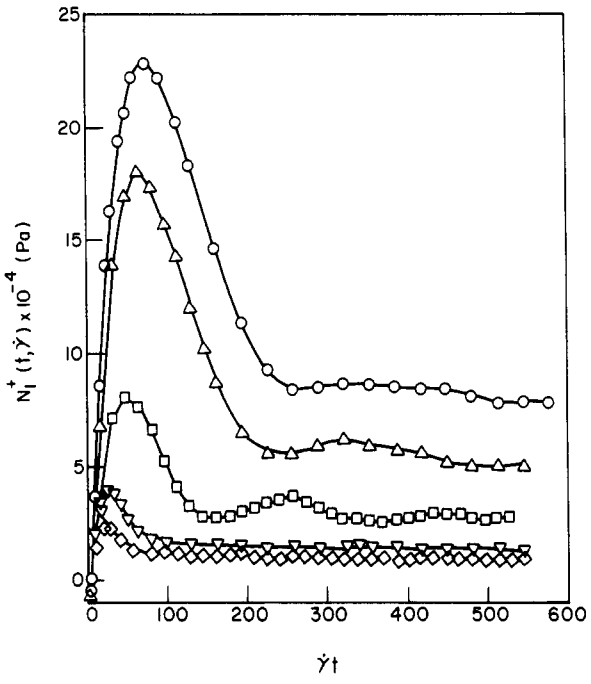

Figure 10. Plots of $N_1^+(t,\dot{\gamma})$ versus $\dot{\gamma}t$ for PSHQ10 samples at 140 °C for $\dot{\gamma} = 0.536\ s^{-1}$: (○) sample A; (△) sample B; (□) sample C; (▽) sample D; (◇) sample E.

both $\sigma^+(t,\dot{\gamma})$ and $N_1^+(t,\dot{\gamma})$ during transient shear flow are characteristic of LCPs in general[13–15,22,41–45] and are attributed to the presence of polydomains, which existed in the PSHQ10 specimen before being subjected to a start-up shear flow. It is believed that such large stresses are needed to break up the polydomains (i.e., piled domain textures).

Effect of Molecular Weight on the Steady Shear Flow Properties of PSHQ10 in the Nematic Region. In investigating the effect of deformation history on the steady shear flow properties of PSHQ10 in the *nematic* region, we applied a series of shear flows to a specimen by

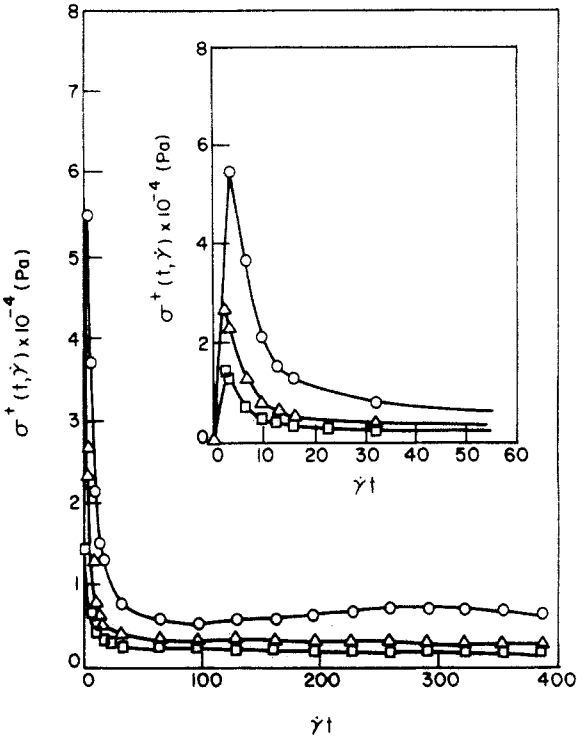

Figure 11. Plots of $\sigma^+(t,\dot\gamma)$ versus $\dot\gamma t$ for sample C at $\dot\gamma = 0.536$ s^{-1} for various temperatures: (○) 130 °C; (△) 140 °C; (□) 150 °C.

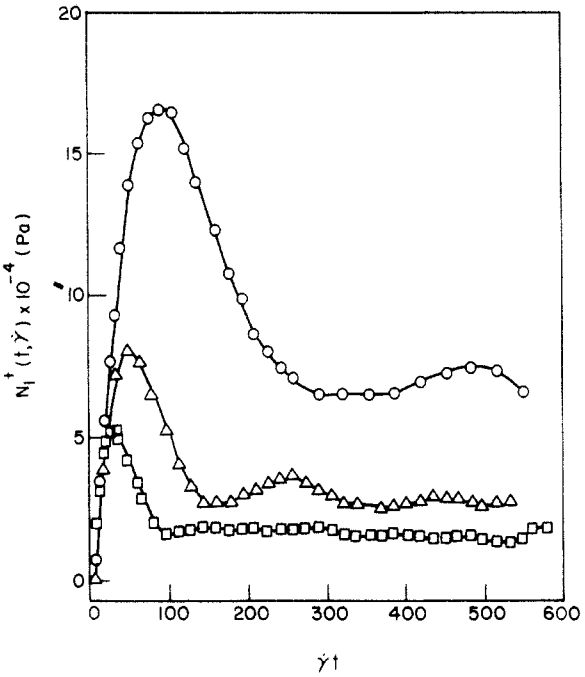

Figure 12. Plots of $N_1^+(t,\dot\gamma)$ versus $\dot\gamma t$ for sample C at $\dot\gamma = 0.536$ s^{-1} for various temperatures: (○) 130 °C; (△) 140 °C; (□) 150 °C.

increasing shear rate stepwise and at each shear rate we waited until a steady state was attained. Figure 13a gives plots of log η versus log $\dot\gamma$ for five PSHQ10 samples at 140 °C in the *first* shear-rate sweep experiment. It can be seen in Figure 13a that shear-thinning behavior is persistent over the entire range of $\dot\gamma$ tested. However, as can be seen in Figure 13b, when the same specimens were subjected to a *second* shear-rate sweep experiment after a 1-h rest period, they exhibit a Newtonian plateau region (i.e., zero-shear viscosity η_0 at low $\dot\gamma$ and shear-thinning behavior as $\dot\gamma$ increases, as often observed in flexible homopolymers. The following observations are worth noting in Figure 13: (1) the steady shear viscosity of PSHQ10 increases with increasing molecular weight and

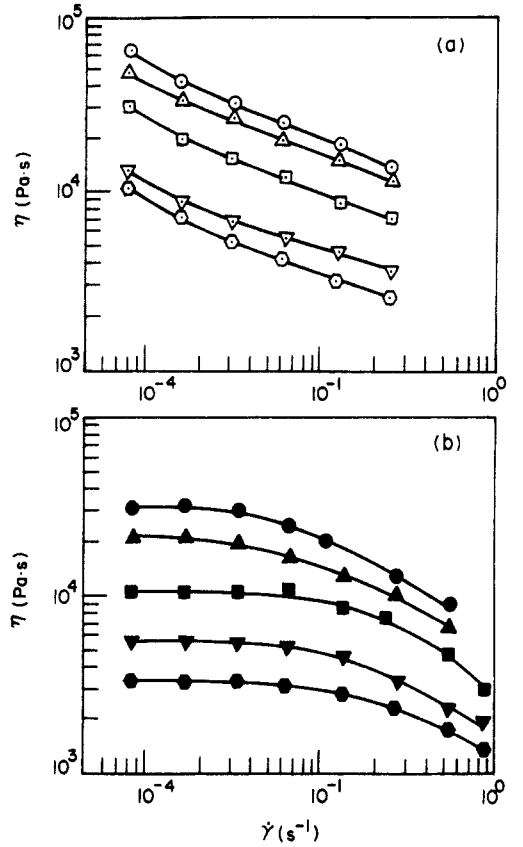

Figure 13. (a) Plots of log η versus log $\dot\gamma$ in the *first* shear-rate sweep experiment (open symbols) and (b) plots of log η versus log $\dot\gamma$ in the *second* shear-rate sweep experiment (filled symbols) for PSHQ10 samples at 140 °C: (○, ●) sample A; (△,▲) sample B; (□,■) sample C; (▽,▼) sample D; (◎,◉) sample E.

(2) *preshearing* has a pronounced effect on the steady shear viscosity.

The dependence of zero-shear viscosity η_0 on molecular weight M of *presheared* PSHQ10 specimens (the data points given in Figure 13) is given in Figure 14, from which,using a regression analysis, we obtain the following relationship:[32]

$$\eta_0 \propto M^6 \tag{2}$$

As mentioned above, owing to the rather small variations of molecular weight tested in this study, the 6th power of molecular weight appearing in eq 2 must be regarded as an approximation.

It should be mentioned that the Doi theory predicts[18]

$$\eta_0 \propto M^6 \frac{(1-S)^4(1+S)^2(1+2S)(1+1.5S)}{(1+0.5S)^2} \tag{3}$$

where S is the order parameter which is zero in the *isotropic* phase and unity in the state of *perfect* alignment. Note that for $S = 0$ eq 3 gives $\eta_0 \propto M^6$. Since the value of S is expected to increase with increasing M at a given temperature, η_0 would *not* be directly proportional to M^6 in the *nematic* region of TLCP. At present, however, we have no information as to how S might vary with M. Note further that in the derivation of eq 3 a mathematical approximation (often referred to as a *decoupling approximation*) was made in treating the term $\mathbf{D}:\langle\mathbf{uuuu}\rangle$ that appears in the system of equations, i.e., $\mathbf{D}:\langle\mathbf{uuuu}\rangle \approx \mathbf{D}:\langle\mathbf{uu}\rangle\langle\mathbf{uu}\rangle$ was used, where $\mathbf{D}$ is the rate-of-deformation tensor and $\mathbf{u}$ is the unit vector. If a higher order approximation is introduced to $\mathbf{D}:\langle\mathbf{uuuu}\rangle$, eq 3 would have a different dependency on S. Nevertheless, it is very encouraging to observe that, within experimental uncer-

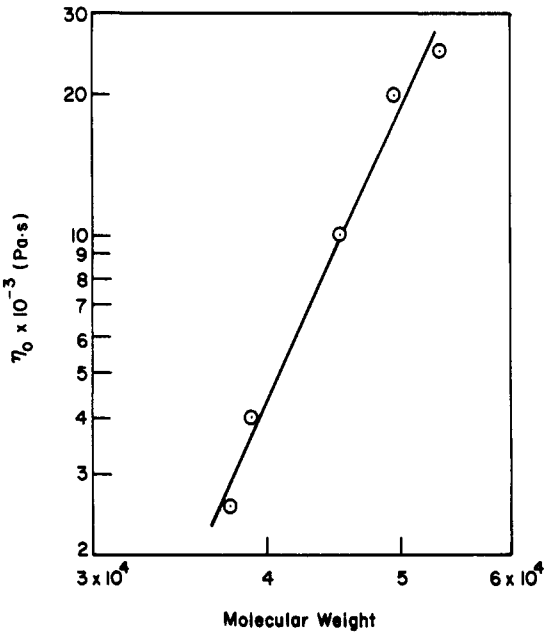

Figure 14. Plots of log η_0 in the nematic region at 140 °C versus M_w for PSHQ10 samples, where the values of η_0 were obtained in the *second* shear-rate sweep experiment.

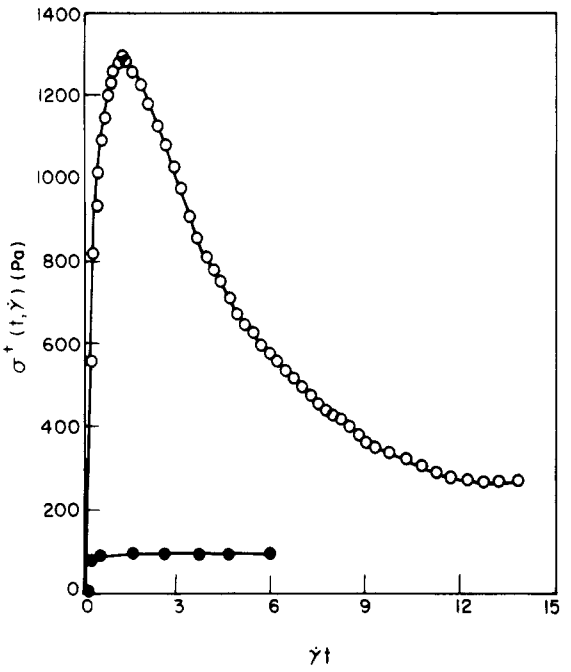

Figure 15. Comparison of $\sigma^+(t,\dot\gamma)$ versus $\dot\gamma t$ plots in the *first* shear-rate sweep experiment (open circles) with those in the *second* shear-rate sweep experiment (filled circles) for sample C, where the *second* shear-rate sweep experiment was conducted after a 1-h rest time upon cessation of the *first* shear-rate sweep experiments. The measurement temperature was 140 °C, and the applied shear rate was 0.0085 s^{-1}.

tainties, the experimental results for the dependence of η_0 on M, presented above for PSHQ10 in the *nematic* state, are reasonably close to Doi's prediction.

The significant decrease in the shear-rate dependence of η by *preshearing* PSHQ10 samples, observed in Figure 13, can be explained by Figure 15, which shows a dramatic difference in the transient shear stress ($\sigma^+(t,\dot\gamma)$ upon startup of shear flow, where the open circles denote $\sigma^+(t,\dot\gamma)$ in the *first* shear-rate sweep experiment and the filled circles denote $\sigma^+(t,\dot\gamma)$ in the *second* shear-rate sweep experiment, both sheared at $\dot\gamma = 0.0085\ s^{-1}$. It should be mentioned that the *second* shear-rate sweep experiment was performed after a 1-h rest period. The results

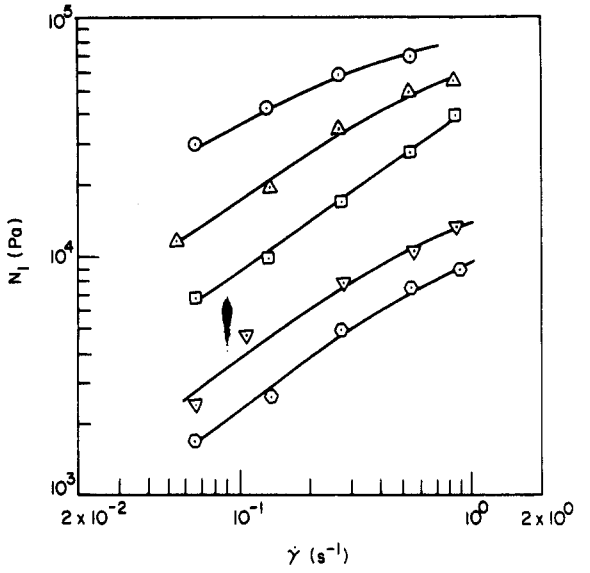

Figure 16. Plots of log N_1 versus log $\dot\gamma$ for PSHQ10 samples at 140 °C in the *second* shear-rate sweep experiment: (⊙) sample A; (▲) sample B; (⊡) sample C; (▼) sample D.; (⊙) sample E.

presented in Figure 15 suggest that the polydomains, which had existed in the specimen after being cooled from the isotropic region, were broken up during the *first* shear-rate sweep experiment and thus virtually *no* overshoot was observed in the *second* shear-rate sweep experiment.

Figure 16 gives plots of log N_1 versus log $\dot\gamma$, which were obtained using the *presheared* PSHQ10 samples at 140 °C (i.e., after the first shear-rate sweep experiment). Note in Figure 16 that N_1 increases with molecular weight. Using regression analysis of the data given in Figure 16, we obtain the relationship between N_1 and $\dot\gamma$:

$$N_1 \propto \dot\gamma^n \tag{4}$$

where n varies from 0.6 to 0.73 depending upon the samples used and the average value of n is about 0.67, which is rather small as compared to that for flexible homopolymers ($N_1 \propto \dot\gamma^2$).[19,20] Also, applying a regression analysis to the data given in Figure 16, we obtain the following relationship between N_1 and M:

$$N_1 \propto M^{6.7} \tag{5}$$

It should be mentioned that the Doi theory predicts[18,46]

$$N_1 \propto \dot\gamma M^6 \frac{S(1-S)^{1.5}(1+2S)^{0.5}(1+1.5S)}{(1+0.5S)^2} \tag{6}$$

for rigid-rod-like macromolecules. It is of interest to observe in eq 6 that $N_1 \propto \dot\gamma$, which is reasonably close to the experimental results given by eq 4. Note that, although eq 6 contains a factor M^6, it should be understood that N_1 will *not* be directly proportional to M^6 because, as mentioned above, the order parameter S would depend on the molecular weight M. At present we have no information as to how S might vary with M. Moreover, the dependence of N_1 on S will be different from that in eq 6 if a higher order closure approximation for $\mathbf{D}\langle\mathbf{uuuu}\rangle$ is used. Note that eq 6 was derived using the *decoupling* approximation for $\mathbf{D}\langle\mathbf{uuuu}\rangle$, i.e., $\mathbf{D}:\langle\mathbf{uuuu}\rangle \approx \mathbf{D}:\langle\mathbf{uu}\rangle\langle\mathbf{uu}\rangle$. Note further than some of the physical assumptions (e.g., initially, a spatially uniform distribution of the directors; the macromolecules consist of rigid rods) made in the Doi theory are not directly applicable to PSHQ10, which is a semiflexible thermotropic polymer melt, having initially a spatially nonuniform distribution of the liquid-crystalline phase. Thus caution must be taken

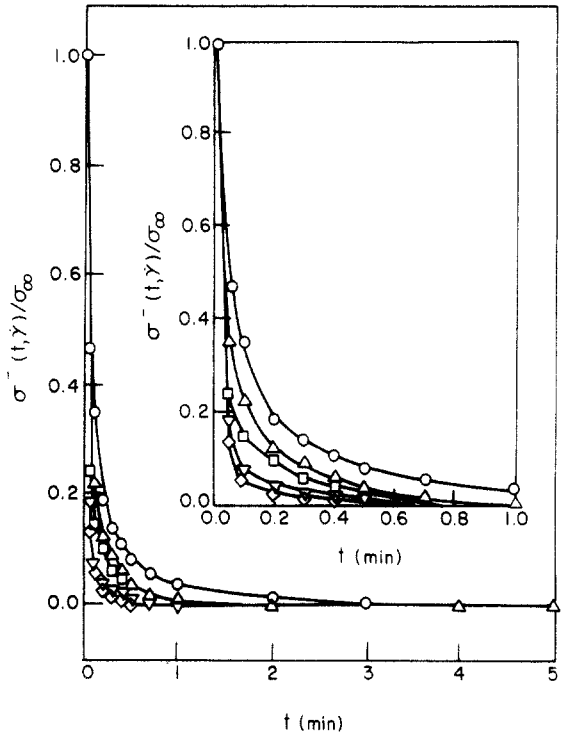

Figure 17. Decay of shear stress $\sigma^-(t,\dot\gamma)$ with time upon cessation of steady shear flow at $\dot\gamma = 0.27\ s^{-1}$ for PSHQ10 samples at 140 °C: (○) sample A; (△) sample B; (□) sample C; (▽) sample D; (◇) sample E.

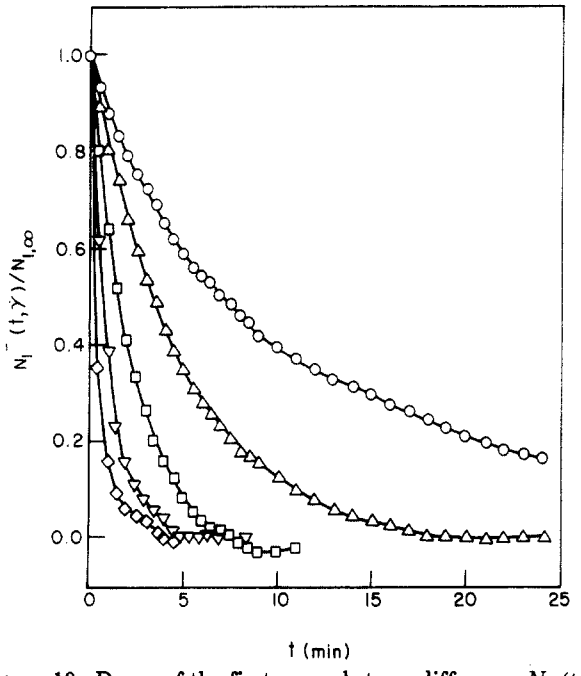

Figure 18. Decay of the first normal stress difference $N_1^-(t,\dot\gamma)$ with time upon cessation of steady shear flow at $\dot\gamma = 0.27\ s^{-1}$ for PSHQ10 samples at 140 °C: (○) sample A; (△) sample B; (□) sample C; (▽) sample D; (◇) sample E.

when attempting to interpret the experimental results presented above using the Doi theory. Nevertheless it is very encouraging to observe that the Doi theory captures the essential features observed in the present experimental study.

Effect of Molecular Weight on the Stress Relaxation of PSHQ10 after Cessation of Steady Shear Flow. The effect of molecular weight on the stress relaxation of PSHQ10 after cessation of steady shear flow can be observed in Figures 17 and 18, where shear stress decay $\sigma^-(t,\dot\gamma)$ and the first normal stress difference decay

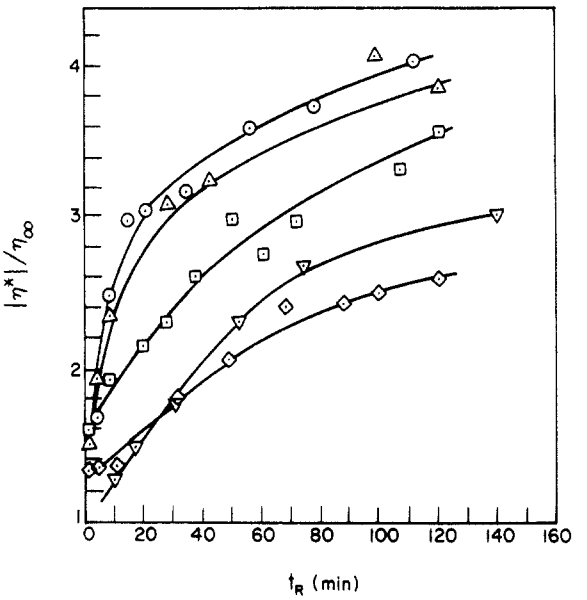

Figure 19. Plots of $|\eta^*|/\eta_\infty$ versus rest time t_R at 140 °C, where η_∞ denotes the steady shear viscosity just before cessation of steady shear flow at $\dot\gamma = 0.27\ s^{-1}$; (○) sample A; (▲) sample B; (□) sample C; (▽) sample D; (◇) sample E.

$N_1^-(t,\dot\gamma)$, respectively, for five PSHQ10 samples at 140 °C are given after cessation of a steady shear flow at $\dot\gamma = 0.27\ s^{-1}$. The following observations are worth noting in Figures 17 and 18: (1) the rate of decay of both $\sigma^-(t,\dot\gamma)$ and $N_1^-(t,\dot\gamma)$ decreases with increasing molecular weight of the specimen; (2) the rate of decay of $N_1^-(t,\dot\gamma)$ is much lower than that of $\sigma^-(t,\dot\gamma)$; (3) for certain samples (C–E) N_1 goes through *negative* values before reaching a positive valued steady state. It would seem possible that we might have observed negative values of $N_1(t,\dot\gamma)$ also for samples A and B if we had waited a longer period after cessation of steady shear flow.

The unusually long relaxation time required for PSHQ10 to attain steady-state values for shear stress and normal stress difference, after cessation of steady shear flow, is believed to be characteristic of TLCPs in general. We hasten to point out that the rate of stress decay and the relaxation time, after cessation of steady shear flow, would depend on the applied shear rate and measurement temperature, since they in turn control the morphological state of the specimen.

Effect of Molecular Weight on the Structural Recovery of PSHQ10 after Cessation of Steady Shear Flow. As mentioned in the Experimental Section, in the present study we monitored "structural recovery," after cessation of steady shear flow, in terms of $|\eta^*|$ of the PSHQ10 specimens by applying small-amplitude oscillatory deformations (for a strain of 0.02 and an angular frequency of 0.075 rad/s). The rationale behind this approach lies in that such small-amplitude oscillatory deformations would affect *little* the morphology of the specimen under test.

Figure 19 gives plots of $|\eta^*|/\eta_\infty$ versus rest time (t_R) for five PSHQ10 specimens at 140 °C after cessation of steady shear flow at $\dot\gamma = 0.27\ s^{-1}$. In preparing Figure 19 the steady shear viscosity (η_∞) at $\dot\gamma = 0.27\ s^{-1}$ was used as a reference for each specimen. It can be seen in Figure 19 that the rate of "structural recovery" increases with increasing molecular weight PSHQ10, suggesting that the morphological state at the end of the steady shear flow applied was different for specimens having different molecular weight. Quantitative analysis of the morphological state (i.e., domain textures) of a PSHQ10 specimen

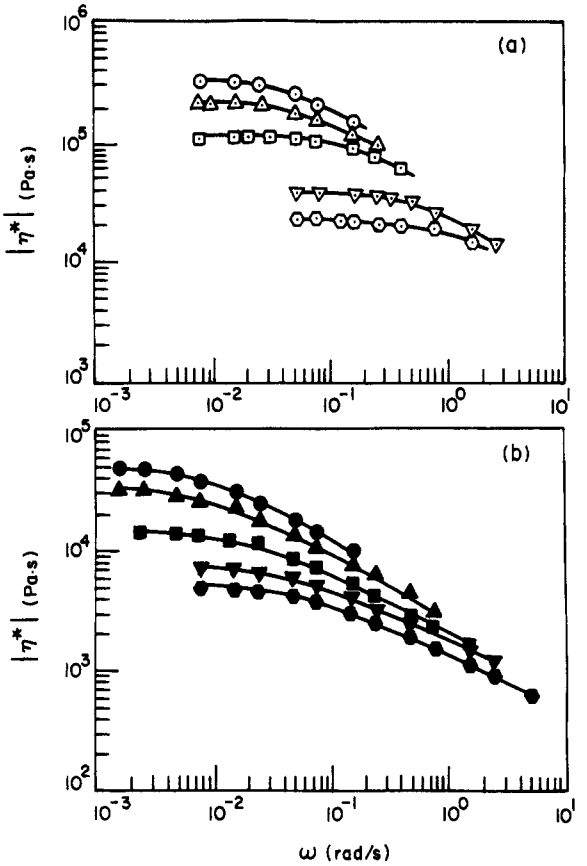

Figure 20. (a) Plots of log $|\eta^*|$ versus log ω before being subjected to steady shear flow (open dotted symbols) and (b) plots of log $|\eta^*|$ versus log ω *after* being subjected to steady shear flow for PSHQ10 samples at 140 °C followed by structural recovery for a period of 3 h (filled symbols): (⊙,●) sample A; (▲,▲) sample B; (⊡,■) sample C; (▼,▼) sample D; (◇,◆) sample E.

after being subjected to steady shear flow is beyond the scope of the present study and will be dealt with in a future investigation.

Effect of Molecular Weight on the Oscillatory Shear Flow Properties of PSHQ10 after Being Subjected to Steady Shear Flow. In this study we also investigated the oscillatory shear flow properties of PSHQ10, which had been subjected to steady shear flow followed by structural recovery. Figure 20 gives plots of log $|\eta^*|$ versus log ω for five PSHQ10 samples at 140 °C *before* being subjected to steady shear flow (Figure 20a) and after being subjected to steady shear flow at $\dot{\gamma} = 0.27$ s^{-1} followed by a rest period of 3 h (Figure 20b). It can be seen in Figure 20 that *preshearing* decreased considerably the $|\eta^*|$ of the PSHQ10 specimens.

Using the data obtained for G' and G'' as a function of ω for PSHQ10 samples, which had been subjected to steady shear flow and then put to rest for a period of 3 h, plots of log G' versus log G'' were prepared and they are given in Figure 21. A comparison of Figure 21 with Figure 8 (open dotted symbols) reveals that the application of steady shear flow has a profound influence on the shape of the log G' versus log G'' plots, suggesting that the domain textures of PSHQ10 samples were different after the application of steady shear flow. Specifically, after a PSHQ10 sample was subjected to steady shear flow, log G' versus log G'' plots (see Figure 21) have a more or less linear correlation, whereas there is a significant curvature in the terminal region of log G' versus log G'' plots for the samples before being subjected to steady shear flow (see Figure 8). The difference observed in the shape of log G' versus log G'' plots between Figure 8 and Figure 21 is

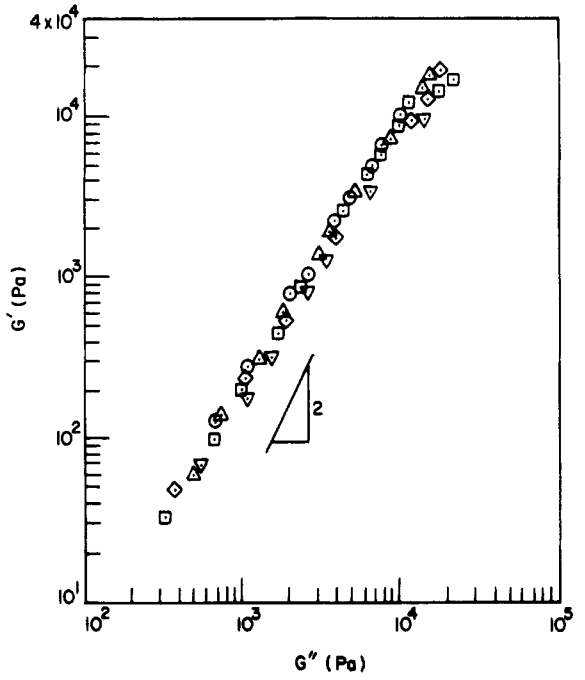

Figure 21. Plots of log G' versus log G'' for PSHQ10 samples at 140 °C *after* being subjected to steady shear flow at $\dot{\gamma} = 0.27$ s^{-1} followed by structural recovery for a period of 3 h: (⊙) sample A; (▲) sample B; (⊡) sample C; (▼) sample D; (◇) sample E.

attributable to the differences that existed in the morphological state (i.e., domain texture) of the samples. We can thus conclude that plots of log G' versus log G'' are very sensitive to variations in the morphological state of TLCPs.

Concluding Remarks

In this study we investigated the effects of molecular weight on the rheological behavior of an aromatic thermoplastic polyester (PSHQ10) in both the isotropic and nematic regions. The following conclusions can be drawn from the present study: (1) We have found that the dependence of shear viscosity on molecular weight is much stronger for PSHQ10 than for flexible homopolymers, which is in qualitative agreement with the Doi theory. (2) When subjected to transient start-up shear flow, the higher the molecular weight of PSHQ10, the greater the values of stress overshoot, and after cessation of shear flow, the higher the molecular weight of PSHQ10, the slower the stress relaxation and also the greater the structural recovery. (3) We found that when using a *fresh* specimen, PSHQ10 did not exhibit Newtonian viscosity at low shear rates, while *presheared* specimens did. In other words, *preshearing* has a profound influence on the rheological behavior of PSHQ10 in the nematic state. We infer from this experimental observation that *preshearing* broke up the polydomains that had existed in the fresh specimen before being sheared.

The molecular weight dependence of the rheological properties reported in this study must be tested further by varying the molecular weight of PSHQ10 with a wider range and, also, using other types of TLCP. Since it is a well-established fact today that polydispersity greatly influences the rheological properties of a polymer, it is desirable to have monodisperse (or nearly monodisperse) TLCPs to test rigorously the dependence of the rheological properties of TLCP on molecular weight. Note, however, that polyesters are produced by condensation polymerization, which cannot yield monodisperse polymers. This means that other polymerization methods must be used

to produce monodisperse TLCPs, which is a challenge to polymer chemists.

References and Notes

(1) Jackson, W. J.; Kuhfuss, H. F. *J. Polym. Sci. Polym. Chem. Ed.* **1976**, *4*, 2043.
(2) Wissbrun, K. F. *Br. Polym. J.* **1980**, *13*, 163.
(3) Jerman, R. E.; Baird, D. G. *J. Rheol.* **1981**, *25*, 275.
(4) Prasadarao, M.; Pearce, E. M.; Han, C. D. *J. Appl. Polym. Sci.* **1982**, *27*, 1343.
(5) Gotsis, A. D.; Baird, D. G. *J. Rheol.* **1985**, *29*, 539.
(6) Wissbrun, K. F.; Griffin, A. C. *J. Polym. Sci., Polym. Phys. Ed.* **1985**, *20*, 1835.
(7) Viola, G.; Baird, D. G. *J. Rheol.* **1986**, *30*, 601.
(8) Wunder, S. L.; Ramachandran, S.; Cochanour, C. R.; Weinberg, M. *Macromolecules* **1986**, *19*, 1696.
(9) Done, D.; Baird, D. G. *Polym. Eng. Sci.* **1987**, *27*, 816.
(10) Irwin, R. S.; Swine, W.; Gardner, K. H.; Cochanour, C. R.; Weinberg, M. *Macromolecules* **1989**, *22*, 1065.
(11) Wissbrun, K. F.; Kiss, G.; Cogswell, F. N. *Chem. Eng. Commun.* **1987**, *53*, 149.
(12) Gonzalez, J. M.; Minoz, M. E.; Cortazar, M.; Santamaria, A.; Pena, J. *J. Polym. Sci., Part B: Polym. Phys.* **1990**, *28*, 1533.
(13) Driscoll, P.; Masuda, T.; Fujiwara, K. *Macromolecules* **1991**, *24*, 1567.
(14) Cocchini, F.; Nobile, M. R.; Acierno, D. *J. Rheol.* **1991**, *35*, 1171.
(15) Guskey, S. M.; Winter, H. H. *J. Rheol.* **1991**, *35*, 1191.
(16) Schneider, H.; Stocker, A.; Korn, M.; Krischeldorf, H. R.; Percec, V. *Mol. Cryst. Liq. Cryst.* **1991**, *196*, 57.
(17) Papkov, S. P.; Kulichikhin, V. G.; Vinogradov, V. G.; Malkin, Y. D. Ya. *J. Polym. Sci., Polym. Chem. Ed.* **1974**, *12*, 1753.
(18) Doi, M. *J. Polym. Sci., Polym. Phys. Ed.* **1981**, *19*, 229.
(19) Ferry, J. D. *Viscoelastic Properties of Polymers*, 3rd ed.; Wiley: New York, 1980.
(20) Doi, M.; Edwards, S. F. *The Theory of Polymer Dynamics*; Clarendon Press: Oxford, U.K., 1986.
(21) Kim, S. S.; Han, C. D. *Macromolecules* **1993**, *26*, 3176.
(22) Kim, S. S.; Han, C. D. *J. Rheol.* **1993**, *37*, 847.
(23) Kim, S. S.; Han, C. D. *J. Polym. Sci., Part B: Polym. Phys.*, in press.
(24) Kim, S. S.; Han, C. D. *Polymer*, in press.
(25) Furukawa, A.; Lenz, R. W. *Makromol. Chem., Macromol. Symp.* **1986**, *2*, 3.
(26) Blumstein, A.; Vilasagar, S.; Ponrathnam, S.; Clough, S. B.; Blumstein, R. B.; Maret, G. *J. Polym. Sci., Polym. Phys. Ed.* **1982**, *20*, 877.
(27) Majnusz, J.; Catala, J. M.; Lenz, R. W. *Eur. Polym. J.* **1983**, *19*, 1043.
(28) Blumstein, R. B.; Stickles, E. M.; Gautheir, M. M.; Blumstein, A.; Volino, F. *Macromolecules* **1984**, *17*, 177.
(29) Percec, V.; Tomazos, D.; Pugh, C. *Macromolecules* **1989**, *22*, 3259.
(30) Laus, M.; Sante Angeloni, A.; Galli, G.; Chiellini, E. *Macromolecules* **1992**, *25*, 5901.
(31) Cox, W. P.; Merz, E. H. *J. Polym. Sci.* **1958**, *28*, 619.
(32) In order to facilitate our discussion here in comparison with theoretical prediction, we use M instead of M_w.
(33) Doi, M. *J. Phys. (Paris)* **1975**, *36*, 607.
(34) Doi, M.; Edwards, S. F. *J. Chem. Soc., Faraday Trans. 2* **1978**, *74*, 918.
(35) Han, C. D.; Jhon, M. S. *J. Appl. Polym. Sci.* **1986**, *32*, 3809.
(36) Han, C. D.; Kim, J. K. *Polymer* **1993**, *34*, 2533.
(37) Lin, Y. G.; Winter, H. H. *Macromolecules* **1988**, *21*, 2439; **1991**, *24*, 2877.
(38) Han, C. D.; Kim, J. *J. Polym. Sci., Part B: Polym. Phys.* **1987**, *25*, 1741.
(39) Han, C. D.; Kim, J.; Kim, J. K. *Macromolecules* **1989**, *22*, 383.
(40) Han, C. D.; Baek, D. M.; Kim, J. K. *Macromolecules* **1990**, *23*, 561.
(41) Metzner, A. B.; Prilutski, G. M. *J. Rheol.* **1986**, *30*, 661.
(42) Doppert, H. J.; Picken, S. J. *Mol. Cryst. Liq. Cryst.* **1987**, *153*, 109.
(43) Mewis, J.; Moldenaers, P. *Mol. Cryst. Liq. Cryst.* **1987**, *153*, 291.
(44) Grizzuti, N.; Cavella, S.; Cicarelli, P. *J. Rheol.* **1990**, *34*, 1293.
(45) Moldenaers, P.; Yanase, H.; Mewis, J. *J. Rheol.* **1991**, *35*, 1681.
(46) The factor $1 + 1.5S$ appearing in the numerator of eq 6 is missing in eq 6.20 of ref 18.